Width distribution for (2+1)-dimensional growth and deposition processes

Zoltán Rácz and Michael Plischke

Physics Department, Simon Fraser University, Burnaby, British Columbia, Canada V5A 1S6

(Received 21 July 1994)

Nonequilibrium growth processes are frequently characterized by the width $w(L,t)$ of the active zone, where t is the time elapsed since the start of the process and L is the spatial interval over which the measurement is carried out. Quite generally, $w(L,t)$ obeys a scaling form $w(L,t) \sim L^\zeta f(tL^{-z})$, and many workers have attempted to determine the dynamic universality class of such processes by a measurement of the exponents ζ and z. In this paper, we calculate the steady-state width distribution $P(w^2)$ for several three-dimensional growth processes and show that, expressed in a suitable form, $P(w^2)$ can be used to distinguish between different possible universality classes. We also reanalyze experimental data obtained by scanning-tunneling or atomic-force microscopy and show that $P(w^2)$ provides valuable information on the nature of a growth process.

I. INTRODUCTION

A number of nonequilibrium processes such as the growth of films by molecular beam epitaxty (MBE) or other deposition processes, the etching of materials by ion bombardment, the invasion of porous media by fluids, and many others display scaling behavior in space and time similar to that found at equilibrium critical points. An important aspect of such nonequilibrium processes is the existence of an active zone in which growth occurs. Generically, the width of this active zone grows as a function of time and is controlled, in the long time limit, only by the physical dimensions of the system and one finds that the expectation value of the width $w(L,t)$ of the active zone obeys the scaling form [1]

$$\langle w(L,t) \rangle = L^\zeta f(tL^{-z}), \qquad (1.1)$$

where the scaling function has the asymptotic form $f(x) \to$ const as $x \to \infty$ and $f \to x^{\zeta/z}$ as $x \to 0$. In (1.1) the quantity L is the distance over which the width is measured (in simulations, often the size of the sample) and t is the time since the beginning of the process. The exponents ζ and z or $\beta = \zeta/z$ are frequently measured (in experiment or in simulations of discrete models) in an attempt to determine the *universality class* of a nonequilibrium growth process. While this can be done in principle, there are frequently difficulties and ambiguities due to crossover effects. A more detailed characterization of the active zone is provided by real-space correlation functions and by the structure factor. However, while these are easily calculated in a simulation, they are not always available to an experimentalist. Thus, it is of interest to find other more detailed descriptions of the interface or active zone of a nonequilibrium process. In this paper, we argue that the probability distribution for the width $P(w^2)$ in the limit $t \gg L^z$ provides significantly more information than simply the width $\langle w \rangle$ and can be used to identify universality classes.

In the following discussion, we confine ourselves to situations in which particles are deposited onto a two-dimensional substrate and where the growing film is free of voids or overhangs. The surface of the resulting solid-on-solid (SOS) model can therefore be described in terms of a single-valued function $h(\mathbf{r},t)$, where $\mathbf{r}$ is a point on the substrate and h is the height of the surface above the substrate. This restriction is mostly for convenience. It is commonly assumed to be appropriate for a description of MBE and is liberal enough to also allow the discusssion of models that fall into the Kardar-Parisi-Zhang (KPZ) [2] universality class. The mean square width is then given by

$$\langle w^2(L,t) \rangle = \frac{1}{N_s} \sum_s \frac{1}{L^2} \sum_{\mathbf{r}} \left[h_s(\mathbf{r},t) - \bar{h}_s \right]^2, \qquad (1.2)$$

where N_s refers to the number of samples in a simulation or the number of equivalent patches of dimension L of a surface in a set of experimental measurements and $\bar{h}_s$ is the average height of the patch above the substrate. Clearly, if there is a sufficiently large number of such equivalent patches, or samples, one can also construct a histogram for the probability distribution $P(w^2)$. In earlier work, Foltin et al. [3] and Plischke et al. [4] have shown that for certain (1+1)-dimensional models, w^2 depends on only a single length scale and, therefore, that $P(w^2)$ can be written as

$$\langle w^2 \rangle P(w^2) = \Phi \left(w^2 / \langle w^2 \rangle \right) \qquad (1.3)$$

in the steady state. Furthermore, they found that the scaling function Φ is a universal characteristic of a given growth process. In this paper, we extend this approach to (2+1)-dimensional systems which have considerably more diversity. We also compare the function Φ obtained for several simple models of MBE to atomic-force and scanneling-tunneling microscopy scans of MBE grown materials.

The structure of this paper is as follows. In Sec. II, we review some of the models that have been used to describe nonequilibrium growth processes. Section III

contains a description of how the function Φ can be calculated for various continuum models. In Sec. IV, we compare the calculated Φ with simulations of models that are well known to be in the same universality class as the continuum models mentioned above. We relate this approach to experiment in Sec. V and conclude with a short discussion in Sec. VI.

II. CONTINUUM AND DISCRETE MODELS FOR NONEQUILIBRIUM GROWTH PROCESSES

In this section, we discuss several Langevin equations that have been used to model growth and deposition processes as well as discrete models, suitable for Monte Carlo calculations, that have the same scaling behavior as these Langevin equations.

A. Kardar-Parisi-Zhang–Edwards-Wilkinson equation and the single-step model

Two of the early but still widely useful continuum models of growth and deposition models are the Edwards-Wilkinson (EW) [5] and the KPZ [2] model. The KPZ model is defined through the Langevin equation:

$$\frac{\partial h(\mathbf{r},t)}{\partial t} = \nu\nabla^2 h(\mathbf{r},t) + \frac{\lambda}{2}(\nabla h(\mathbf{r},t))^2 + \eta(\mathbf{r},t), \quad (2.1)$$

where $\nu > 0$ and η represents Gaussian white noise. The Edwards-Wilkinson equation is obtained when $\lambda = 0$ in (2.1). These equations were originally proposed as models for sedimentation (EW) and for growth processes like the Eden model (KPZ) in which growth occurs in a direction locally perpendicular to the existing interface. Both are also useful in other contexts, including as models for MBE [6]. In the context of thin film growth, the parameter ν is a surface tension parameter which may be microscopically due to evaporation, or to nonequilibrium effects such as slope-dependent surface diffusion currents [7]. The coefficient λ multiplies a term that produces a growth velocity that depends on the magnitude of the slope and we, therefore, expect this term to be present if there are voids and overhangs in the growing film or, as mentioned above, if the growth direction is locally perpendicular to the interface. The linear Edwards-Wilkinson equation is exactly solvable and is characterized in (2+1) dimensions by $z = 2$ and $\zeta = 0$ (logarithmic dependence of the average width on L). The KPZ equation is still not fully understood in the (2+1)-dimensional case. Computer simulations of models that are expected to be in the KPZ universality class (and certainly are in one dimension) yield [8] $\zeta \approx 0.385$ and $z \approx 1.615$.

A discrete model that interpolates between the EW and KPZ limits is the so-called single-step model [9,10]. In this model, particles of height 2 are deposited or evaporated according to the following rules: (i) only sites which are by one unit of height lower than their nearest neighbors are eligible for deposition; conversely, evaporation can only occur at sites that are one unit higher than

their neighbors; (ii) deposition occurs with probability p to one of the eligible sites, evaporation with probability $1-p$. The substrate is a square lattice and initially $h(\mathbf{r},0)$ is either 0 or 1 so that the nearest neighbors of sites of height 0 are all of height 1. The parameter p determines the universality class of this process: for $p = 0.5$ the surface is, on the average, stationary and the KPZ term vanishes in the continuum description; for any $p \neq 0.5$, the long-wavelength behavior crosses over to a "strong coupling fixed point" with the exponents quoted above [10]. We use this model for illustrative purposes in the next section.

B. Mullins-Herring equation and curvature-driven dynamics

Next, we consider some of the models that have been proposed specifically for the description of growth by molecular beam epitaxy. It is generally assumed that, under ideal MBE conditions, particles deposited on the substrate do not reevaporate and relax through surface diffusion. Moreover, it is also generally assumed that there are no voids or overhangs. The continuum description of MBE growth then begins with a conservation law [11]:

$$\frac{\partial h(\mathbf{r},t)}{\partial t} + \nabla\cdot\mathbf{j}([h]) = \eta(\mathbf{r},t), \quad (2.2)$$

where the noise term η is due to fluctuations in the beam intensity. In the simplest version of this model, the diffusion current $\mathbf{j}$ is assumed to depend only on the curvature of the surface: $\mathbf{j} \propto \nabla(\nabla^2 h(\mathbf{r},t))$, leading to the linear Mullins-Herring (MH) equation [12]:

$$\frac{\partial h(\mathbf{r},t)}{\partial t} = -\nu_4\Delta\Delta h(\mathbf{r},t) + \eta(\mathbf{r},t) . \quad (2.3)$$

As is the case for the EW equation, this Langevin equation is exactly solvable and, when the noise term η is nonconserved Gaussian white noise, leads to the exponents $\zeta = 1$, $z = 4$ in (2+1) dimensions.

There has been considerable confusion in the literature with regard to the continuum description of discrete models designed to model MBE. Originally, it was thought that models of the Wolf-Villain type [13,14] fell into the universality class of Eq. (2.3). However, recent work [15] has shown convincingly that these models have a more complicated scaling behavior than that predicted by Eq. (2.3). There are two discrete models that seem to clearly fall into the universality class of (2.3). One is the $n = 2$ model of Siegert and Plischke [6], the other is the "larger curvature model" of Kim and Das Sarma [16] and Krug [17]. Both of these models have the feature that the probability of a particle hopping to a neighboring site depends only on the discretized form of the local curvature. In the following sections, we will use the $n = 2$ model to compare $P(w^2)$ for the discrete and continuum models and we, therefore, briefly describe it here. In this model, the energy of a configuration is given by $E = \sum_{\langle\mathbf{r},\mathbf{r}'\rangle}[h(\mathbf{r}) - h(\mathbf{r}')]^2$, where $\mathbf{r},\mathbf{r}'$ are nearest-

neighbor sites on the substrate. The transition rate W for the process $h(\mathbf{r}) \to h(\mathbf{r}) - 1$, $h(\mathbf{r}') \to h(\mathbf{r}') + 1$ is then given by $\tau W = [\exp\{\beta \Delta E\} + 1]^{-1}$, where τ^{-1} is an attempt frequency, ΔE the change in energy due to the hop, and β is the inverse of the temperature. It is easy to see that with the quadratic energy function, W depends only on the gradient of the local curvature.

C. Conserved KPZ equation and Arrhenius dynamics

There have been a number of proposed modifications of Eq. (2.3) that incorporate the lowest order relevant nonlinearities. Because of the conservation law (2.2) the KPZ term is forbidden. However, a conserved version of the KPZ term is allowed and was originally included by Villain [11]. This yields the Langevin equation:

$$\frac{\partial h(\mathbf{r},t)}{\partial t} = -\nu_4 \Delta \Delta h(\mathbf{r},t) + \frac{\lambda}{2}\Delta \left[\boldsymbol{\nabla} h(\mathbf{r},t)\right]^2 + \eta(\mathbf{r},t).$$

$$(2.4)$$

Because of the nonlinearity, this equation is not exactly solvable. At the one-loop order of a dynamic renormalization group analysis [18], the predicted exponents are $\zeta = \frac{2}{3}$ and $z = \frac{10}{3}$. There is at present no compelling evidence that this equation describes a particular discrete model exactly. The exponents of a simple nearest-neighbor SOS model with Arrhenius dynamics are, however, quite close to these predicted values [19] and, in the following sections, we shall use this model in connection with Eq. (2.4). The energy function in this model is $E = \epsilon \sum_{\langle \mathbf{r},\mathbf{r}'\rangle} |h(\mathbf{r}) - h(\mathbf{r}')|$ and transition rates are calculated in the following way [20]. The coordination number n_L of a particle attempting to hop is given by the number of nearest-neighbor columns of height greater than or equal to that of the hopping particle and an attempted hop is accepted with probability $W = \exp\{-\beta n_L \epsilon\}$. In the next section, we shall discuss the calculation of the distribution $P(w^2)$ for the continuum models presented above.

III. CALCULATION OF THE WIDTH DISTRIBUTION FUNCTION

Foltin et al. [3] and Plischke et al. [4] have shown how the distribution function $P(w^2)$ can be calculated exactly for the one-dimensional versions of the EW and MH equations and we shall only outline the method here. In two dimensions, we are unable to evaluate $P(w^2)$ in closed form but it can be put into a form useful for numerical evaluation, using the methods of [3,4]. We begin by writing $P(w^2)$ in terms of a path integral:

$$P(w^2) = \mathcal{N} \int D[h]\delta\left(w^2 - \overline{h^2} - \bar{h}^2\right)$$

$$\times \exp\left\{-\int d^2 r \mathcal{H}[h]\right\},$$

$$(3.1)$$

where $\mathcal{N}$ is a normalization constant and where the effective Hamiltonian $\mathcal{H}$ will be defined later. In Eq. (3.1), the functional integral is assumed to be carried out over all configurations and

$$\overline{h^2} = \frac{1}{L^2}\int d^2 r h^2(\mathbf{r}).$$

It is useful also to define the generating function for the distribution P:

$$G(\lambda) \equiv \int_0^\infty dx P(x)e^{-\lambda x}$$

$$= \mathcal{N}\int D[h]\exp\left\{-\int d^2 r\left[\mathcal{H}[h] + \frac{\lambda}{L^2}h^2(\mathbf{r})\right]\right\},$$

$$(3.2)$$

where, without loss of generality, we have taken $\bar{h} = 0$.

The generating function is easily calculated if $\mathcal{H}[h]$ is a quadratic function of h. We, therefore, begin by considering the two linear Langevin equations [Eq. (2.1) with $\lambda = 0$ and (2.3)]. In these cases, the effective Hamiltonian is known. For the EW equation,

$$\mathcal{H}_{\rm EW} = \frac{g}{2}\left(\nabla h\right)^2$$

$$(3.3)$$

where g is a constant of dimension $[L^{-2}]$, whereas for the MH equation, we have

$$\mathcal{H}_{\rm MH} = \tilde{g}\left(\nabla^2 h\right)^2,$$

$$(3.4)$$

where, in this case, the constant $\tilde{g}$ is dimensionless.

A. Mullins-Herring equation

We begin with this case since its analysis is straightforward as compared to the EW equation where divergent sums appear. In the MH case, we proceed by writing

$$h(\mathbf{r}) = \sum_{m,n} c_{mn} e^{2\pi i(mx+ny)/L},$$

$$(3.5)$$

where $m,n = 0, \pm 1, \pm 2, \ldots$, excluding $m = n = 0$ since $\bar{h} = 0$. Inserting this into Eq. (3.2) and writing $c_{mn} = \alpha_{mn} + i\gamma_{mn}$, where α_{mn}, γ_{mn} are real and using $c_{mn} = c^*_{-m-n}$, we obtain the generating function as an infinite product:

$$G(\lambda) = \mathcal{N}\prod_{m,n}{}' \int_{-\infty}^\infty d\alpha_{mn} \int_{-\infty}^\infty d\gamma_{mn} \exp\left\{-(\alpha_{mn}^2\right.$$

$$\left. +\gamma_{mn}^2)\left[\frac{16\pi^4 \tilde{g}}{L^2}(n^2 + m^2)^2 + 2\lambda\right]\right\}$$

$$= \prod_{m,n}{}' \frac{a_{mn}}{\lambda + a_{mn}},$$

$$(3.6)$$

where $a_{mn} = 8\pi^4 \tilde{g}(n^2 + m^2)^2/L^2$. Because $c_{mn} = c^*_{-m-n}$ the values of m,n that appear in (3.6) are given by $m > 0, -\infty < n < \infty$, and $m = 0, 1 \leq n < \infty$, hence the

WIDTH DISTRIBUTION FOR (2+1)-DIMENSIONAL GROWTH ...

notation $\prod'$. The expectation value of the width is given by

$$\langle w^2 \rangle = -\left.\frac{\partial}{\partial \lambda} \ln G(\lambda)\right|_{\lambda=0} = \left(\frac{L^2}{8\pi^4 \tilde{g}}\right) {\sum_{m,n}}' \frac{1}{(m^2+n^2)^2} .$$

(3.7)

The sum over m, n converges rapidly and $\langle w^2 \rangle$ can easily be evaluated to arbitrary accuracy.

To obtain $P(w^2)$, we must invert the Laplace transform (3.2). Formally,

$$P(w^2) = \frac{1}{2\pi i} \int_{-i\infty}^{i\infty} d\lambda\, G(\lambda) e^{\lambda w^2} .$$

(3.8)

Unfortunately, the generating function has an infinite number of poles and, in contrast to the one-dimensional case, we are unable to sum all the residues. However, it is straightforward to construct a sequence of approximations keeping more and more poles. Figure 1 shows the function $\Phi(x) = \langle w^2 \rangle P(w^2)$ plotted as function of the scaled variable $x = w^2/\langle w^2 \rangle$ for three approximations in which the 5, 15, and 31 poles closest to the origin have been retained in the integration. Clearly, the scaled distribution function is converging to a limit function. We estimate that the best approximation is accurate to better than 1% except near $x = 0$, where the function vanishes rapidly and in a singular manner. In this region, Φ is primarily determined by poles far from the origin that have been neglected.

B. Edwards-Wilkinson equation

The Edwards-Wilkinson equation is special in that it is necessary to introduce a short-distance cutoff. This is in marked contrast to the case of the MH equation, where the only length scale necessary for a complete description of the width distribution is the average value of the width itself. This emergence of a second significant length is familiar from other situations such as the Gaussian approximation to critical phenomena: This model is ill defined without the explicit introduction of a cutoff. Nevertheless, we shall see that we can derive interesting results for the function $\Phi(x)$ by taking appropriate limits.

The analog of Eq. (3.6) in the EW case reads,

$$G(\lambda) = {\prod_{m,n}}' \frac{2\pi^2 g(n^2+m^2)}{\lambda + 2\pi^2 g(n^2+m^2)} ,$$

(3.9)

and the average of w^2 is given by

$$\langle w^2 \rangle = \frac{1}{2\pi^2 g} {\sum_{m,n}}' \frac{1}{n^2+m^2} \equiv \frac{S}{2\pi^2 g} .$$

(3.10)

The problem with this calculation is now clear: $\langle w^2 \rangle$ diverges unless the sum S in (3.10) is restricted to a finite number of terms. This can be enforced by introducing a microscopic cutoff (discretizing the system). We take this cutoff to be unity and consider a system of finite
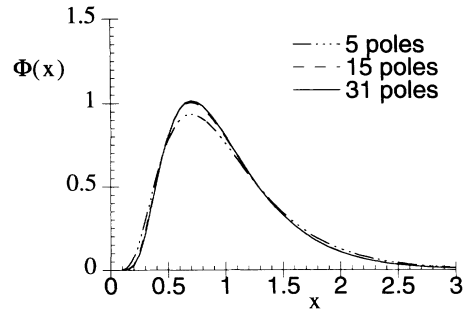

FIG. 1. Approximate calculation of $\Phi(x)$ for the MH model on the basis of Eq. (3.8) using the residues of n poles closest to the origin with $n = 5$, 15, and 31.

size L. Then (3.10) is well defined since $|n|, |m| \leq L$ and $S = S(L)$ is finite. Consequently, we can write the scaling function in the form

$$\Phi(x) = \langle w^2 \rangle P(w^2)$$
$$= \int_{-i\infty}^{i\infty} \frac{dz}{2\pi i} e^{zx} {\prod_{n,m}}' \left(1 + \frac{zS^{-1}}{n^2+m^2}\right)^{-1} .$$

(3.11)

The scaling function now depends not only on x but also on L (through S). In the limit $L \to \infty$, we have $S \sim \ln L \to \infty$ and, thus, S^{-1} in Eq. (3.11) can be used as a small parameter in the following approximation. We exponentiate the product in (3.11) and expand the sum of logarithms in the exponential. We then find

$$\Phi(x) = \int_{-i\infty}^{i\infty} \frac{dz}{2\pi i} \exp\left\{ z(x-1) + \frac{a_2}{2}z^2 \right. $$
$$\left. + \cdots + \frac{a_k}{k} z^k + \cdots \right\} ,$$

(3.12)

where

$$a_2 = \frac{1}{S^2} {\sum_{n,m}}' \frac{1}{(n^2+m^2)^2}$$

(3.13)

and, in general,

$$a_k = \frac{(-1)^k}{S^k} {\sum_{n,m}}' \frac{1}{(n^2+m^2)^k} .$$

(3.14)

Since the sums in (3.13) and (3.14) are finite when $L \to \infty$, one can see that all $a_k \to 0$ and, for an infinite system, we find a δ-function distribution:

$$\lim_{L\to\infty} \Phi(x) = \delta(x-1) .$$

(3.15)

For finite but large L, the leading corrections to the δ function are obtained by retaining only the term proportional to a_2 in Eq. (3.12). This results in a Gaussian distribution,

$$\Phi(x) \approx \frac{1}{\sqrt{2\pi a_2}} \exp\left\{ -\frac{(x-1)^2}{2a_2} \right\} ,$$

(3.16)

where $a_2 = c(\ln L)^{-2}$ with $c = 2.99\ldots/\pi^2$. Thus, for large systems, the function $\Phi(x)$ asymptotically becomes a Gaussian centered at $x = 1$ with a width that approaches zero in the thermodynamic limit as $(\ln L)^{-1}$. The maximum of this distribution $\Phi_{\max}$ grows with system size as $\Phi_{\max} \sim \sqrt{\pi/6}\,\ln L$.

C. phenomenological Approach: k^γ models

In the case of nonlinear Langevin equations, such as the KPZ equation (2.1) or the conserved KPZ equation (2.4), we do not know the effective Hamiltonian. In this section we carry out a purely *ad hoc* calculation of the function $\Phi(x)$ on the basis of the following phenomenological considerations. The width of the interface in the steady state can be related to an integral over the structure factor $S(\mathbf{k}) = \left\langle \hat{h}(\mathbf{k})\hat{h}(-\mathbf{k}) \right\rangle$, where $\hat{h}(\mathbf{k})$ is the Fourier transform of $h(\mathbf{r})$. This function generically diverges as $|k|^{-\gamma}$ at long wavelength, where $\gamma = 2\zeta + d$ with d the substrate dimension. For the linear EW and MH models, $\mathcal{H}[\hat{h}(\mathbf{k})] \propto S^{-1}(\mathbf{k})$ and the poles that enter into the inverse Laplace transform (3.8) are precisely at $\lambda = -bS^{-1}(\mathbf{k})$, where b is a constant and $\mathbf{k} = 2\pi(n,m)/L$. Therefore, we conjecture that a nonlinear Langevin equation that has a structure factor which diverges at long wavelength with a clean (i.e., crossover-free) power law $|k|^{-\gamma}$ will have a width distribution given by

$$P(w^2) = \int_{-i\infty}^{i\infty} \frac{d\lambda}{2\pi i} e^{\lambda w^2} \prod_{\mathbf{k}}' \frac{bS^{-1}(\mathbf{k})}{\lambda + bS^{-1}(\mathbf{k})} \cdot \quad (3.17)$$

Writing $\lambda = z\left\langle w^2 \right\rangle^{-1}$ with $\left\langle w^2 \right\rangle = b^{-1}\sum_{\mathbf{k}}' S(\mathbf{k})$, we arrive at the form

$$\Phi(x) = \int_{-i\infty}^{i\infty} \frac{dz}{2\pi i} e^{zx} \prod_{\mathbf{k}}' \frac{1}{zS(\mathbf{k})[\sum_{\mathbf{q}} S(\mathbf{q})]^{-1} + 1} \cdot \quad (3.18)$$

We remark that $\Phi(x)$ does not depend on the constant b.

The calculation then proceeds as for the MH model with a finite number of poles retained in the evaluation of the contour integral (3.18). In Fig. 2, we show successive approximations to $\Phi(x)$ calculated in this manner for $\gamma = 3$. This value of γ was chosen because it is quite close to the value of $10/3$ appropriate for the conserved KPZ equation (2.4) and closer still to the value measured [19] for the case of Arrhenius dynamics in three dimensions. The convergence to a limit function is substantially slower than for $\gamma = 4$ (MH model) but the final form of the scaling function can easily be inferred from the curves plotted.

We make no attempt to justify this procedure formally. Certainly, we do not expect it to be exact or to yield reasonable results in cases where there is crossover between different power laws in $S(\mathbf{k})$. However, as we shall see in the next section, it does provide a very good fit to $\Phi(x)$ for the Arrhenius model and a reasonable representation of Φ for the single-step model.
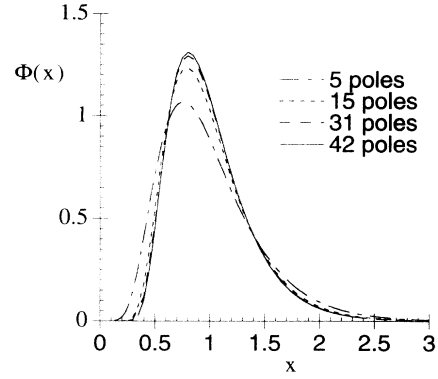

FIG. 2. Calculation of $\Phi(x)$ for a phenomenological effective Hamiltonian with $\mathcal{H}[h(\mathbf{q})] = q^3|h(\mathbf{q})|^2$. The approximation scheme is the same as in Fig. 1.

IV. COMPARISON WITH COMPUTER SIMULATIONS

In this section, we show the width distribution for a number of growth models and, where possible, compare with the calculations of Sec. III.

A. KPZ–Edwards-Wilkinson class

We begin with the single-step model described above. When the deposition rate p is not equal to 0.5, this model has the property that $S(\mathbf{k}) \sim |\mathbf{k}|^{-\gamma}$ with $\gamma \approx 2.70$; when $p = 0.5$, $\gamma = 2.0$, the EW value. In Fig. 3, we show $\Phi(x)$ for several substrate sizes for $p = 1.0$ and for $L = 128$ for $p = 0.9$. The collapse of the data to a single curve is quite remarkable. We remark that since $\Phi(x)$ is normalized and collapses extremely well at both large and small x, it must also have a universal maximum value and the seeming scatter of points near the peak is simply due to sampling errors. Also shown in this figure is the phenomenological calculation of Φ by the methods
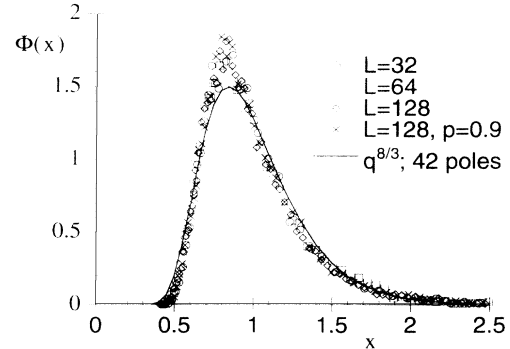

FIG. 3. The universal function $\Phi(x)$ for the single-step model with $p = 1.0$ and 0.9. For each value of L, the data were obtained from a minimum of 100 samples. The solid line is the phenomenological Φ calculated on the assumption that $S(q) \sim |q|^{-8/3}$, appropriate for the KPZ equation in $d = 2$.

of Sec. III C with $\gamma = 8/3$, appropriate for the single-step model. In this calculation we have retained the 42 poles closest to the origin in the integral. At this level of approximation, the fit is not perfect but the peak is in the correct location and successive approximations with more poles show a very encouraging convergence toward the simulations. We have also simulated the single-step model with $p = 0.75$ for systems up to $L = 256$. For this value of p the crossover between the Edwards-Wilkinson and KPZ universality classes is clearly visible in the structure factor. However, even for a system of size 256×256 the effective exponent γ determined from the smallest q vectors is only about 2.5, i.e., the crossover is extremely slow. However, the function Φ does seem to be approaching the same limiting function as in Fig. 3, supporting the conclusion that there is a single scaling function for the KPZ universality class.

The scaling function Φ for the case $p = 0.5$ contrasts sharply with those obtained for a moving interface. As mentioned above, the case $p = 0.5$ is well described by the EW equation and should, therefore, produce a scaling function that approaches a δ function centered at $x = 1$ as $L \to \infty$ [Eq. (3.16)]. In Fig. 4, we display $\Phi(x)$ for $L \leq 128$. The scaling function clearly becomes more narrow for increasing L. A fit of the peak height to the form $\Phi_{\max} = a + b \ln L$ produces $b \approx 0.7$, in very satisfactory agreement with the prediction of (3.16).

B. Mullins-Herring class

The driven discrete Gaussian model with surface diffusion governed by Metropolis transition probabilities is known [6] to be in the universality class of the MH equation. In Fig. 5, we show $\Phi(x)$ for this model for a 32×32 substrate, a deposition rate of 0.1 and $\beta\epsilon = 1.0$. Also shown is our best approximation to Eq. (3.8), where we have kept 31 poles in the inverse Laplace transform. The agreement between the two functions is quite good. However, more important is the fact that the function Φ for this case is clearly distinguishable from that of the single-step model or, equivalently, of the two-dimensional KPZ equation. The distribution is considerably broader and cuts off at a much smaller value of x. As we have shown for the one-dimensional version of this class of models [4], the distribution is insensitive to changes in the micro-

FIG. 5. Comparison of the width distribution for the $n = 2$ model for a 32×32 substrate and the best approximation to Eq. (3.8).

scopic growth rules and parameters. Thus even simple measurements, such as the peak height or the value of the small-x cutoff provide a criterion that can be used to assign growth processes to universality classes.

C. Arrhenius dynamics

As a final example, we compute the function $\Phi(x)$ for the SOS model with Arrhenius dynamics described in Sec. II. This discrete model has exponents close to those of the conserved KPZ equation (2.4). Therefore, we have another example of the variation of Φ with universality class, as well as a check on the phenomenological analytical calculations of Sec. III C. The results are shown in Fig. 6 for $L = 32$ and for the 42-pole approximation to Eq. (3.17). The agreement between the simulation and the phenomenological approximation is excellent, providing support for the conjecture that the function $\Phi(x)$ is determined primarily by the long-wavelength behavior of the heigh-height correlation function. The function Φ lies between the corresponding distribution of the KPZ model and the MH model as one would expect, given that the exponent γ is intermediate between those of the KPZ and MH equations.

V. RELATION TO EXPERIMENT

With the development of scanning-tunneling (STM) and atomic-force microscopy (AFM) as standard tool of condensed matter physics it has become possible to characterize surfaces in unprecedented detail. In particular,
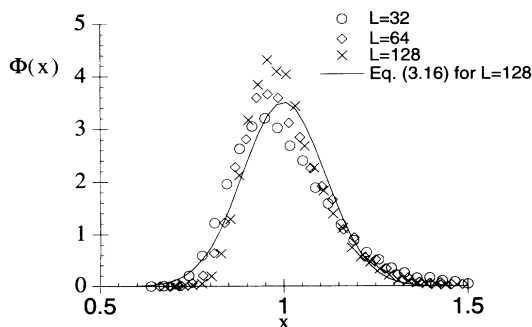

FIG. 4. $\Phi(x)$ for the single-step model for $p = 0.5$. This model is in the EW universality class and the growth of the peak height and decrease of the width as function of L is consistent with the predictions of Eq. (3.16).
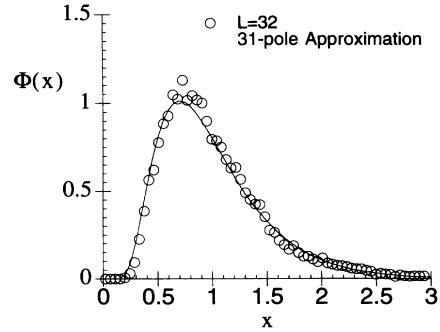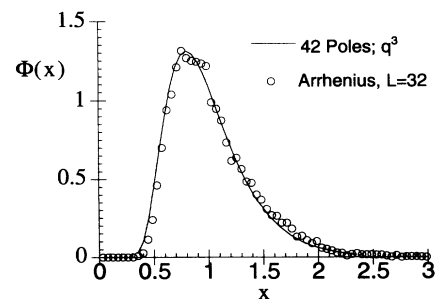

FIG. 6. Comparison of $\Phi(x)$ for the SOS model with Arrhenius dynamics for $L = 32$ with the best approximation of Fig. 2.

it is now possible to measure $h(\mathbf{r})$ over a wide range of $\mathbf{r}$ of a film grown to a particular thickness. From such a measurement one can extract the width of the interface, as has been done, [21,22] but also more detailed information such as the probability distribution of the height [21] and the function Φ as we now show.

The discussion of the previous sections has been for the width distribution in the *steady state*. In computer simulations on finite systems, the steady state is easy to recognize—one simply waits until the expectation value $\langle w^2 \rangle$ has saturated. In an experiment, films are typically grown to some thickness ranging from one to several hundred nanometers. Given that the substrate size L is invariably much larger than the thickness, these films are globally far from the steady state. It is necessary then to characterize experimental samples in terms of a horizontal correlation length $\xi(t)$ where t is the thickness of the film. For distances $|\mathbf{x} - \mathbf{x}'| \ll \xi$ or wave vectors $k \gg \xi^{-1}$, the height-height correlations or the structure factor have attained thickness-independent values. Conversely, for larger distances or shorter wavelengths, the film is still in a nonequilibrium state. To calculate the function Φ from an STM or AFM scan one can proceed as follows. We assume that the film profile exists as an array $h(x, y)$. The correlation length ξ can then be estimated by calculating the function

$$g(\mathbf{r}) = \sum_{\mathbf{r}'} \left[h(\mathbf{r} + \mathbf{r}') - \overline{h} \right] \left[h(\mathbf{r}') - \overline{h} \right] / (N_s w^2), \quad (5.1)$$

where N_s is the number of sites $\mathbf{r}'$ included in the summation and w^2 is the square of the width calculated over the entire data set. The function $g(\mathbf{r})$ goes to zero at distances of order ξ. Once ξ is known, the substrate can then be divided into square patches of linear dimension $L \le \xi$. Each of these patches yields a value for the width and these "independent" samples can then be combined to produce $P(w^2)$ and from this Φ.

This procedure is, in principle, straightforward. However, there is a potential problem when one applies it to small patches because the free-boundary conditions, which allow tilted interfaces, are different from the periodic boundary conditions and large-size (thermodynamic) limit used in the theoretical calculation of Φ. We do not expect that this will cause a problem when the patch is large enough. At the moment, however, we have no criterion for determining a minimum patch size, where boundary conditions become irrelevant [23].

We have carried out the analysis described above for sample $B3$ of reference [21]. This sample consists of an AFM scan of a 5 μm$\times$5 μm surface, with a horizontal resolution of 10 nm for a 42 nm thick film of CuCl grown on a substrate of CaF$_2$ The data consists of a 512×512 set of values of $h(x, y)$. The correlation length ξ of this sample, calculated from the point at which $g(r)$ of (5.1) crosses zero, was estimated to be between 200 nm and 300 nm. We then divided the data into bins of size 8×8, 16×16, and 32, yielding from 4096 to 256 values of w^2 which were then used to calculate Φ. Our experience with the discrete models discussed in previous sections indicates that $\Phi(x, L)$ does not depend on the substrate size L at all unless there is a crossover, as in the single-step model.

In the case of sample $B3$, however, the function Φ is quite different for the three different values of L and we are, therefore, unable to draw firm conclusions regarding the universality class of this system. We show it in Fig. 7 for $L = 32$ together with the universal functions for KPZ, MH, and Arrhenius dynamics. Clearly, none of these models provides a convincing fit to the data although the MH model does seem marginally better than the others. However, this method can only yield reasonable results if the function Φ is insensitive to the choice of patch size L at least for some range [24].

We have also carried out the same analysis for the STM data of Palasantzas and Krim [22]. These data consist of five 1500 nm$\times$1500 nm scans over the surface of a 702 nm thick Ag film grown on a quartz substrate. Each data set consists of 400×400 values of $h(x, y)$. Henceforth, we take the horizontal spacing of 3.75 nm to be our unit of length. The steady-state exponent ζ for this sample is $\zeta = 0.82 \pm 0.05$ [22]. The results for the scaling function are shown in Fig. 8 for $L = 5$, 10, and 40. The correlation length of this sample, again defined to be the first zero of $g(r)$ is $\xi \approx 25$, so that for the smaller values of L the data should collapse to a single curve characteristic of the steady state. For the larger value of L there may still be nonequilibrium contributions to Φ. Indeed, the data for $L = 5$ and 10 collapse quite nicely, especially in the large x regime. Rermarkably, these data are fit very well by the function Φ of the *one-dimensional* MH model. At the moment, we have no eplanation for this. We conjecture that there may be some anisotropy in the deposition or surface diffusion process that manifests itself in anisotropy in the steady-state width distribution at least on length scales of 20–40 nm. For the larger value of L the data, as already mentioned, are not fully equilibrated. Nevertheless, they are described better by the two-dimensional MH model than by any of the other models for which we have calculated Φ.

VI. DISCUSSION

In this paper we have provided compelling evidence that the scaled probability distribution Φ of the width of an interface in the steady state of a nonequilibrium growth process is a universal function characteristic of that process. In particular, this function seems to be determined entirely by the exponent γ that characterizes the divergence of the static structure factor at small q,
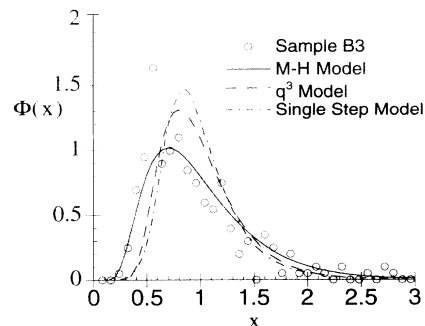

FIG. 7. Comparison of the experimental data of [21], and the universal function Φ for the MH, q^3, and single-step models.
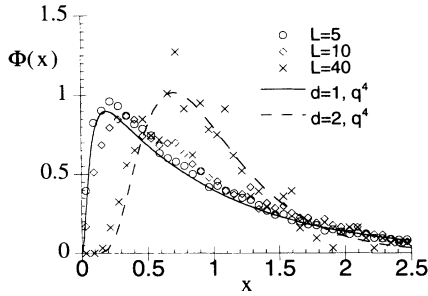
FIG. 8. The function $\Phi(x)$ calculated for $L = 5$, 10, and 40 nm for a 702 nm thick Ag film [22]. The curves correspond to the one-dimensional and two-dimensional MH model.

or equivalently by the exponent ζ that characterizes the dependence of the width on L. Thus, it appears that a single static exponent determines the shape of $\Phi(x)$ and, consequently, that this function can only be used to distinguish the static universality classes of surface growth. It should be noted, however, that in all the models of surface growth discussed above, as well as in others currently under investigation, the dynamics and statics are strongly coupled: Their dynamic exponent z is related to the static exponent through a scaling law [9,13,25,26]. Provided this scaling law is known, $\Phi(x)$ completely determines the universality class of the process. As far as

the experimental determination of $\Phi(x)$ is concerned, we have demonstrated that this function is experimentally accessible through AFM or STM measurements of the profile of a film. Thus, we believe that this distribution function may provide an important tool for the determination of universality classes of growth processes.

Clearly, there are a number of directions for further investigation. As we saw in the previous section, experimental data on Ag films for small L are more consistent with a *one-dimensional* model for the steady-state distribution than with any of the two-dimensional models that we have studied. This makes it important to understand the role of spatial anisotropy in this formalism. As well, it would be useful to have more extensive data on systems with larger correlation lengths so that the parameter L in the analysis of the data can be varied over a larger range.

ACKNOWLEDGEMENTS

[1] F. Family and T. Vicsek, J. Phys. A **18**, L75 (1985).

[2] M. Kardar, G. Parisi, and Y. Zhang, Phys. Rev. Lett. **56**,889 (1986).

[3] G. Foltin, K. Oerding, Z. Rácz, R.L. Workman, and R.K.P. Zia, Phys. Rev. E **50**, 639 (1994).

[4] M. Plischke, Z. Rácz, and R.K.P. Zia (unpublished).

[5] S.F. Edwards and D.R. Wilkinson, Proc. R. Soc. London, Ser. A **381**, 17 (1982).

[6] M. Siegert and M. Plischke, Phys. Rev. E **50**, 917 (1994).

[7] J. Krug, M. Plischke, and M. Siegert, Phys. Rev. Lett. **70**, 3271 (1993).

[8] B.M. Forrest and L.-H. Tang, Phys. Rev. Lett. **64**, 1405 (1990).

[9] P. Meakin, P. Ramananlal, L.M. Sander, and R.C. Ball, Phys. Rev. A **34**, 5091 (1986).

[10] D. Liu and M. Plischke, Phys. Rev. B **38**, 4781 (1988); M. Plischke, Z. Rácz, and D. Liu, *ibid.* **35**, 3485 (1987).

[11] J. Villain, J. Phys. (France) I **1**, 19 (1991).

[12] W.W. Mullins, J. Appl. Phys. **28**, 333 (1957); *Metal Surfaces: Structure Energetics and Kinetics* (American Society for Metals, Metals Park, Ohio 1963), p. 17; C. Herring, in *The Physics of Powder Metallurgy*, edited by W.E. Kingston (McGraw-Hill, New York, 1951), p. 143.

[13] D.E. Wolf and J. Villain, Europhys. Lett. **13**, 389 (1990).

[14] S. Das Sarma and P. Tamborenea, Phys. Rev. Lett. **66**, 325 (1991).

[15] M. Schroeder, M. Siegert, D.E. Wolf, J.D. Shore, and M. Plischke, Europhys. Lett. **24**, 563 (1993); M. Plischke, J.D. Shore, M. Schroeder, M. Siegert, and D.E. Wolf, Phys. Rev. Lett. **71**, 2509 (1993).

[16] J.M. Kim and S. Das Sarma, Phys. Rev. Lett. **72**, 2903 (1994).

[17] J. Krug, Phys. Rev. Lett. **72**, 2907 (1994).

[18] Z.-W. Lai and S. Das Sarma, Phys. Rev. Lett. **66**, 2348 (1991).

[19] M. Plischke and M. Siegert (unpublished).

[20] M.R. Wilby, D.D. Vvedensky, and A. Zangwill, Phys. Rev. B **46**, 12 896 (1992); **47**, 16 068 (1993).

[21] W.M. Tong, R.S. Williams, A. Yanase, Y. Segawa, and M.S. Anderson, Phys. Rev. Lett. **72**, 3374 (1994).

[22] G. Palasantzas and J. Krim (unpublished).

[23] As a practical matter, when analyzing experimental data one has to decide whether or not to adjust $h(x,y)$ by removing an overall tilt of the surface on each patch. Such a subtraction imposes "averaged fixed end" boundary conditions the patches. For large patches this subtraction does not affect $\Phi(x)$ but there are some differences for the smaller patches. The results quoted in this paper were obtained using the raw data of [21] and [22] without correcting for tilt. We are indebted to J. Krim for bringing this point to our attention.

[24] There are indications that, due to heteroepitaxy, CuCl grown on CaF_2 substrates forms three-dimensional islands via a Stranski-Krastanov process and, therefore, may not be describable in terms of the simple scaling formalism of kinetic roughening. [R.S. Williams (private communication); W.M. Tong and R.S. Williams (unpublished).]

[25] J. Krug and H. Spohn, in *Solids Far From Equilibrium*, edited by C. Godrèche (Cambridge University Press, Cambridge 1991).

[26] T. Sun, H. Guo, and M. Grant, Phys. Rev. A **40**, 6763 (1989).